analytical chemistry

ARTICLE

pubs.acs.org/ac

Microfluidic Characterization and Continuous Separation of Cells and Particles Using Conducting Poly(dimethyl siloxane) Electrode Induced Alternating Current-Dielectrophoresis

Nuttawut Lewpiriyawong,[†] Kumaravel Kandaswamy,[‡] Chun Yang,*[,†] Volodymyr Ivanov,[‡] and Roman Stocker[§]

[†]School of Mechanical and Aerospace Engineering, Nanyang Technological University, 50 Nanyang Avenue, Singapore 639798

[‡]School of Civil and Environmental Engineering, Nanyang Technological University, 50 Nanyang Avenue, Singapore 639798

[§]Department of Civil and Environmental Engineering, Massachusetts Institute of Technology, 77 Massachusetts Avenue, Cambridge, Massachusetts 02139, United States

Supporting Information

ABSTRACT: This paper presents a poly(dimethyl siloxane) (PDMS) polymer microfluidic device using alternating current (ac) dielectrophoresis (DEP) for separating live cells from interfering particles of similar sizes by their polarizabilities under continuous flow and for characterizing DEP behaviors of cells in stagnant flow. The ac-DEP force is generated by three-dimensional (3D) conducting PDMS composite electrodes fabricated on a sidewall of the device main channel. Such 3D PDMS composite electrodes are made by dispersing microsized silver (Ag) fillers into PDMS gel. The sidewall AgPDMS electrodes can generate a 3D electric field that uniformly distributes throughout the channel height and varies along the channel lateral direction, thereby producing stronger lateral DEP effects over the entire channel. This allows not only easy observation of cell/particle lateral motion but also using the lateral DEP force for manipulation of cells/particles. The former feature is used to characterize the frequency-dependent DEP behaviors of *Saccharomyces cerevisiae* (yeast) and *Escherichia coli* (bacteria). The latter is utilized for continuous separation of live yeast and bacterial cells from similar-size latex particles as well as live yeast cells from dead yeast cells. The separation efficiency of 97% is achieved in all cases. The demonstration of these functions shows promising applications of the microfluidic device.

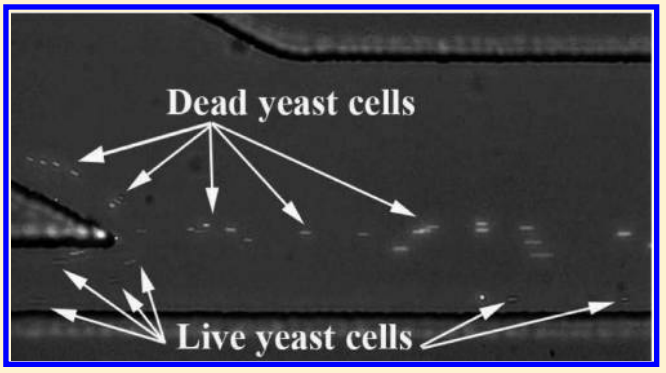

Cell separation is of broad importance in a large number of applications such as biomedical diagnosis in hospitals and environmental monitoring of water quality. Common separation techniques such as flow cytometry and fluorescence-activated cell sorters (FACS) involve bulky and costly instruments, whose operation requires highly trained personnel.[1,2]

With the advancement of microfabrication technology, separation devices for biological diagnosis increasingly undergo development toward miniaturized, portable, and inexpensive devices. Among separation techniques used in microdevices, dielectrophoresis (DEP) is one of the most promising approaches for manipulating and separating microparticles[3,4] and biological particles such as bacteria[5,6] and blood cells.[7−9] DEP is resulted from interactions between an applied nonuniform electric field and induced unevenly distributed dipoles within a polarized cell suspended in a buffer solution. Such interactions can lead to a nonzero coulombic net force on the cell and thus causes its motion.[19] This even occurs without the need to pretreat cell samples. Cells can be manipulated by DEP to move toward high or low electric field regions, depending on the relative polarizability between the cells and their suspending medium.[10]

Since the DEP force magnitude is scaled to the cubic power of cell size, the separation of cells by size is straightforward.[11,12] However, for cells of similar sizes, the separation becomes challenging because the DEP force is only proportional to the relative polarizability between the cells and their suspending medium. Moreover, a suitable electric field frequency is also required to discriminate these cells. Thus, a new microfluidic device is needed to meet these requirements so as to achieve both cell characterization and separation features.

The usual method of creating DEP requiring the nonuniform electric field is through the deposition of thin-film planar electrode arrays on the channel surface of DEP-based microfluidic devices.[13,14] However, the electric field generated in such

Received: September 8, 2011
Accepted: October 29, 2011
Published: October 29, 2011

kind of devices decays exponentially from the surface of the electrodes.[15] As a result, cells located relatively far from the planar electrodes will not experience the DEP force and fail to drift. To enhance DEP force effects, numerous DEP devices with 3D electrodes to generate 3D electric field have been developed and these devices are fabricated using various techniques, such as double planar electrode deposition on both bottom and top substrates,[8] heavy doping of silicon,[16] pyrolysis of SU-8 photoresist,[17] and electroplating of gold.[18] Another important advantage of employing 3D electrodes is to reduce the Joule heating effect in DEP devices.[19,20] Among these devices, there are two main categories of separation methods. The first category employing 3D protruding metal structures in a microchannel such as heavily doped silicon and pyrolyzed SU-8 photoresist captures one type of cells from its binary mixture between 3D electrodes and allows the other to elute first. The second category using double-planar electrodes and electroplated-gold sidewall electrodes typically requires DEP or hydrodynamic focusing and subsequently separates different cells by lateral deflections. However, these microfluidic devices are usually made from glass or silicon and are subject to significant complications in their assemblage to prevent liquid leakage.

With fast development of soft lithography techniques, polydimethylsiloxane (PDMS) is now widely used as the fabrication material of choice in microfluidic devices, owing to several beneficial features, including ease of fabrication and bonding, optical transparency, biocompatibility, and low cost.[21] However, it remains difficult to implement DEP in PDMS-fabricated microfluidic devices because adhesion between metallic electrodes and PDMS is poor.[22] Manually inserting copper electrodes into a PDMS channel[23,24] partially overcomes the problem, but this method is unsuitable for fabrication and also easily causes leakage problem (due to usual mismatch of the thickness of copper sheet and the channel height).

Here we describe a complete polymer microfluidic device that employs AC-DEP via 3D conducting PDMS composites as sidewall electrodes for cell characterization and separation. This approach greatly facilitates (i) the integration of the electrodes (the conducting PDMS composites) with PDMS microstructures and (ii) the assembly of the device through bonding between the PDMS channels, with embedded PDMS composites electrodes, and a glass substrate, involving only oxygen plasma treatment. Furthermore, the device permits easy observation of cell movement within the microchannel and more importantly can generate 3D electric field to allow for extended DEP force effects over the entire channel. As a result, the device can readily manipulate the lateral motion of cells. Such device was successfully used for separation of particles of different sizes.[11] In this study, we demonstrate the applicability of the device for the characterization of the frequency-dependent DEP properties of biological cells and for the continuous separation of live cells from interfering particles and dead cells of similar sizes. DEP behaviors of yeast and bacterial cells were characterized by studying the effect of medium conductivity and ac field frequencies (10 kHz to 80 MHz) in stagnant solutions. For continuous-flow separation, the presented device has dual functions: one is to employ hydrodynamic focusing of sample flow stream to a narrow zone near the sidewall conducting PDMS electrodes where DEP force effects are strong, and the other is to separate live cells (by attractive DEP force) from interfering particles (by repulsive DEP force) based on different DEP polarizabilities.

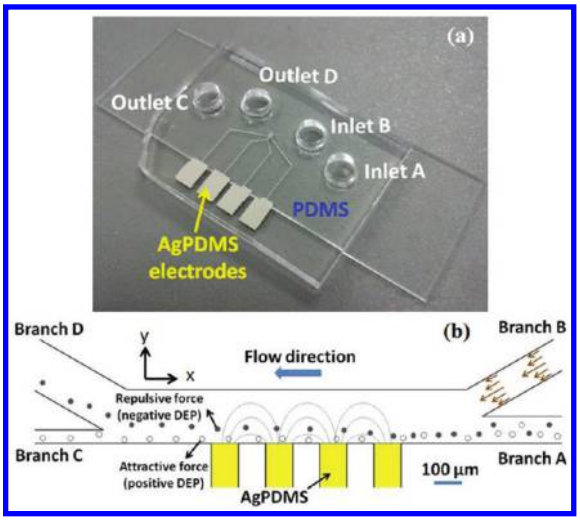

Figure 1. (a) The PDMS-based microfluidic device with sidewall AgPDMS electrodes. (b) Schematic of the continuous separation process for a mixture of two different particles/cells of similar sizes, achieved by (i) hydrodynamic focusing of the sample from branch A toward the electrodes and (ii) DEP forces induced by the AgPDMS electrodes.

MATERIALS AND METHODS

Microfluidic Device Design and Operation for Both Separation and DEP Characterization. Figure 1a shows a microfluidic device, which consists of a 200 μm wide and 1400 μm long main channel with four branch channels that end up in two inlets (A and B) and two outlets (C and D). The widths of the branch channels A, B, C, and D are 100, 115, 50, and 170 μm, respectively. All channels are 40 μm deep. Along one side wall of the main channel, there are four 100 μm wide AgPDMS electrodes, spaced 100 μm apart. All four reservoirs at the inlets and outlets are the same, and each has 4 mm in height and 6 mm in diameter, giving rise to volumetric capacity of about 113 μL. Such large reservoir volume was found to be able to generate steady flow more than 10 min via controlling the liquid level difference.

Figure 1b illustrates the principle of separating a binary particle—cell mixture using DEP together with a flow-focusing approach. The cell transport and flow focusing were controlled by liquid height differences in reservoirs. The reservoirs of all inlets and outlets were first filled with the same NaCl solution, and then liquid in the reservoir of inlet A was replaced by the particle—cell mixture for separation. By using a syringe to suck out liquid (~50 μL) from the two outlets C and D, flow was generated in the channels through the suction effect. The liquid level in the two inlets A and B were maintained so as to achieve hydrodynamic focusing of the sample steaming from inlet A. As a result, inlet B carries a NaCl solution stream to hydrodynamically focus the cells coming from inlet A to transport near the side of the main channel where the AgPDMS electrodes are present to generate strong DEP effects.[11] The total flow rate in the main channel controls the sample velocity and the time available for separation, while the ratio of the flow rates in branches B and A, respectively, determines the degree of hydrodynamic focusing. Particles (shown as solid dots) experience a repulsive DEP force (i.e., negative DEP or nDEP), which is strong enough to overcome the hydrodynamic drag force to generate sufficient lateral migration (along the y direction) and can be guided

to the upper outlet D. Meanwhile, cells (shown as empty dots) experience an attractive DEP force (i.e., positive DEP or pDEP) and hence move toward the lower outlet C.

Because of the fact that the fabricated sidewall electrodes allow for easy observation of cell and particle lateral motion, the device was also used for characterizing DEP behaviors of cells. DEP characterization of cells was performed in stagnant solutions under ac electric field. Prior to experiment, the device was flushed thoroughly with the test medium before injecting cell mixture through inlets A and B. Liquid from outlets C and D was removed to introduce sample mixture to the main channel, and the liquid levels were balanced by using a 50 μL syringe to ensure no motion of sample cells before applying the electric field.

Device Fabrication. The device was fabricated following the same fabrication procedures as presented in our previous work,[11] which describes the soft lithography process together with a method to integrate conducting PDMS electrodes into PDMS microchannels. In brief, after a 40 μm thick SU-8 layer was patterned on a silicon wafer, AZ9260 photoresist was double-coated to obtain a 40−45 μm thick layer. After UV exposure, AZ9260 was developed to create cavities for housing AgPDMS. Conducting paste (AgPDMS) with an electrical conductivity of $\sim 2 \times 10^4$ S/m was made by mixing 1 μm silver (Ag) particles with PDMS gel at a ratio of 85% w/w (above this, the paste could become too powdery). After filling AZ9260 cavities with AgPDMS and removing excessive AgPDMS, the device was heated at 70 °C for 2 h. AZ9260 was then dissolved from the wafer using acetone, followed by ethanol and DI water. PDMS gel was poured on the mold and cured. After the cured PDMS with embedded AgPDMS composite electrodes was peeled, the channel was punched to create four reservoirs and then bonded with a glass substrate using oxygen plasma treatment. Finally, the device is seamlessly integrated with AgPDMS composite electrodes (Figure 1a).

Sample Preparation and Separation Efficiency. Cells of *Saccharomyces cerevisiae* (baker's yeast cells) and *E. coli* DSMZ 1329 (bacterial cells), and two types of particles (Duke Scientific): latex particles (2.9 μm in diameter similar to the size of *E. coli* bacterial cells) and fluorescent latex particles (5 μm in diameter similar to the size of yeast cells) were used in this study. The samples were suspended in NaCl solutions for DEP experiment. The conductivities of suspending media were adjusted to 380 and 600 μS/cm. The conductivity was measured using a conductivity meter (Fisher Scientific AR-20). To prepare yeast cell samples, 50 mg of Baker's yeast (dry form) was suspended in 4 mL of DI water for 1 h for reactivation. The samples were equally divided into two microcentrifuge tubes. In the first tube, a live yeast suspension was centrifuged and transferred into 2 mL of a 380 μS/cm NaCl solution. To prepare dead yeast cells, the yeast sample suspension in the second tube was heated at 80 °C in a water bath for 30 min. The heated cells were stained with 6 μL of propidium iodide (PI) stain (Molecular Probes Inc.) for 30 min in the dark. Then, the dead yeast cells were washed and transferred into 2 mL of a 380 μS/cm NaCl solution. Finally, the live and dead yeast cells were mixed prior to the experiment.

E. coli bacterial cells were grown in a flask containing 100 mL of Luria−Bertani (LB) broth (DifcoTM, Becton Dickinson) in a shaker incubator at 200 rpm and 37 °C. After two 1 mL aliquots were transferred to a microcentrifuge tube, the sample was centrifuged and transferred into 1 mL of a 380 μS/cm NaCl solution. To differentiate them from other particles, the bacterial cells were stained with 1 μL of fluorescent nucleic acid stain SYTO9 (Molecular Probes Inc.) for 30 min at 30 °C in the dark, then washed three times with the 380 μS/cm NaCl solution.

For separation experiments, three suspensions were prepared: (1) live yeast cells and 5 μm fluorescent latex particles in a 380 μS/cm NaCl solution; (2) live bacterial cells stained with SYTO9 and 2.9 μm latex particles in a 380 μS/cm NaCl solution; and (3) live yeast cells and dead yeast cells stained with PI in a 600 μS/cm NaCl solution. Prior to each experiment, a 5% bovine serum albumin (BSA) solution was used to coat the microchannel for ~4 h to prevent adhesion of particles and cells, then thoroughly washed with a NaCl solution to remove BSA. The 5% BSA solution was prepared by dissolving 5 g of A9647 Albumin Bovine Fraction V powder (Sigma-Aldrich) in 100 mL of DI water.

The DEP forces induced by the AgPDMS electrodes were generated by ac voltages supplied by a function generator (Agilent, 33250A), amplified by an amplifier (Piezo System, EPA-102), and monitored by an oscilloscope (HAMEG Instruments, HM 1008). The motion of particles and cells was recorded at 15 frames per second using a CCD camera (Samba, EZ-140 c) mounted on an epifluorescence microscope (Zeiss, Axiostar Plus FL). For experiments in which two types of cells or particles were separated, the separation efficiency was computed as

$$\eta = \left(1 - \frac{R_{\text{loss}}}{R_{\text{A}}}\right) \times 100\%$$

where R_{A} is the number of samples (counted per minute) flowing from inlet A (or the system throughput), and R_{loss} is the number of samples (counted per minute) flowing into the wrong outlet. The throughput is obtained by multiplying the sample velocity and the number of the samples within the traveled distance of a given time. The separation efficiency is averaged over the efficiencies at 1, 2, 3 min after application of the ac field.

THEORETICAL BACKGROUND ON DIELECTROPHORESIS

Dielectrophoresis refers to the motion of a polarized cell in a dielectric medium under an applied nonuniform electric field. Using the dipole moment method, the time-average DEP force acting on a spherical homogeneous cell of radius a suspended in a dielectric medium with permittivity ε_{m} is[10]

$$\langle \vec{F}_{\text{DEP}} \rangle = 2\pi\varepsilon_{\text{m}} a^3 \text{Re}[\underline{K}(\omega)] \nabla |\vec{E}_{\text{rms}}|^2 \quad (1)$$

where $\langle\rangle$ denotes the time-average, Re[] is the real part of a complex number, and $\nabla|\vec{E}_{\text{rms}}|^2$ represents the gradient of the square of the electric field. $\underline{K}(\omega)$ is the complex Clausius-Mossotti (CM) factor,

$$\underline{K}(\omega) = \frac{\underline{\varepsilon}_{\text{cell}} - \underline{\varepsilon}_{\text{m}}}{\underline{\varepsilon}_{\text{cell}} + 2\underline{\varepsilon}_{\text{m}}} \quad (2)$$

where $\underline{\varepsilon}_{\text{cell}}$ is the effective complex permittivity of the cell and $\underline{\varepsilon}_{\text{m}}$ is the complex permittivity of the suspending medium. The CM factor of biological cells such as yeast and bacteria cells can be computed by modeling these cells as consisting of three concentric layers with different permittivities and electrical conductivities[25,26] (Figure S1 in the Supporting Information). When the cell is less polarizable than the medium ($\text{Re}[\underline{K}(\omega)] < 0$), negative DEP (nDEP) pushes the cell away from the high electric field region.

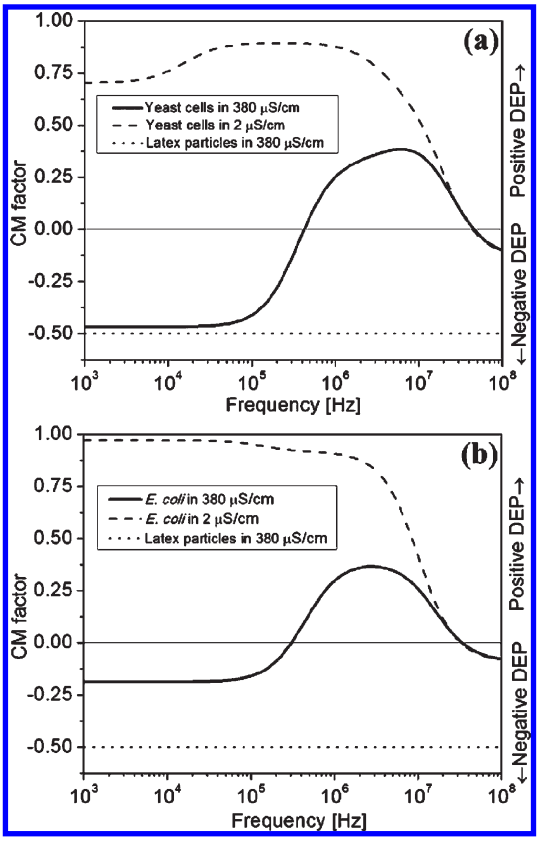

Figure 2. The CM factor as a function of the electric field frequency for a yeast cell (a), an *E. coli* bacterium cell (b) and a latex particle (a and b). The geometrical and electrical properties of yeast and bacterial cells were taken from the literature[26,27] (see the Supporting Information).

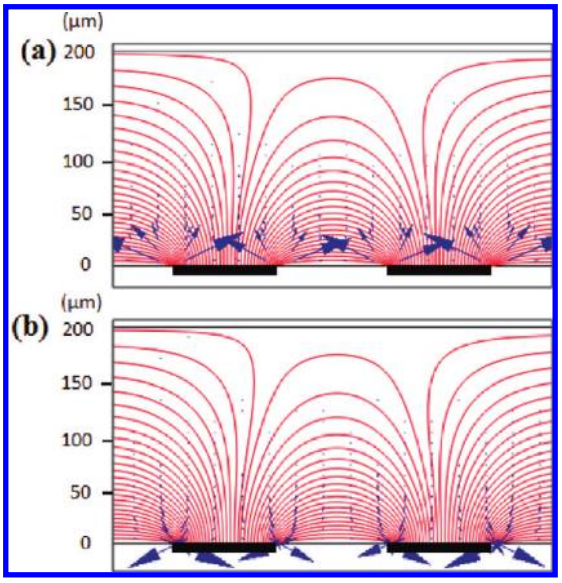

Figure 3. Numerical simulation results for (a) negative and (b) positive DEP forces generated by AgPDMS electrodes (thick black segments). Lines show the contours of the electric field. DEP forces at the boundary are shown by arrows, of length proportional to the strength of the force.

When the cell is more polarizable than the medium ($\mathrm{Re}[\underline{K}(\omega)] > 0$), positive DEP (pDEP) attracts the cell toward the high electric field

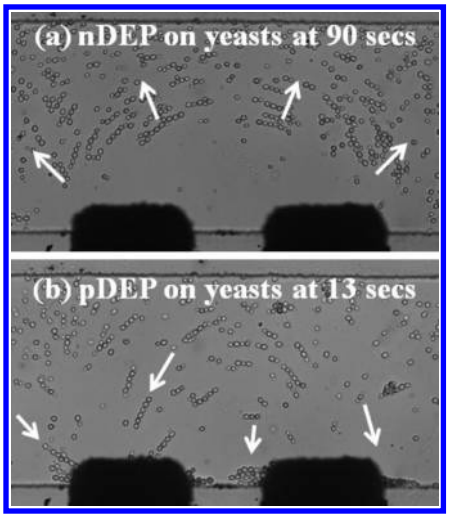

Figure 4. DEP characterization of yeast cells in a 380 μS/cm NaCl solution, in the absence of fluid flow. (a) Repulsion of cells by nDEP under 10 V at 10 kHz after 90 s. (b) Attraction of cells by pDEP after 13 s under 10 V at 10 MHz. Images were obtained with a 20× objective.

region. Figure 2 shows the CM factor as a function of the electric field frequency for yeast and bacterial cells suspended in DI water (2 μS/cm) and in a NaCl solution (380 μS/cm).

The electric field $E = -\nabla\phi$ is related to the electric potential ϕ, which in turn is governed by Laplace's equation ($\nabla^2 \phi = 0$). The boundary conditions are specified according to the microfluidic channel (shown in Figure 1b): the component of the electric field perpendicular to the (nonconducting) PDMS walls is imposed to be zero, the first and third electrodes (from the left, in Figure 1b) have a given electric potential ($\phi = V_{ac}$), and the second and fourth electrodes are electrically grounded ($\phi = 0$).

RESULTS AND DISCUSSION

The electric fields and DEP forces on cells for the same configuration and operating conditions used in the experiments were computed numerically using COMSOL Multiphysics. Figure 3 shows the electric field lines (lines) and the strength of the DEP forces (arrows). When the CM factor is negative (nDEP; Figure 3a), DEP forces point from the electrodes into the fluid, suggesting that cells will experience repulsive forces that push them away from the electrodes. The opposite happens when the CM factor is positive (pDEP; Figure 3b). Near the edges of the AgPDMS electrodes, the highly nonuniform electric field results in a marked increase in the strength of DEP forces, as indicated by the accumulation of electric field lines. The electric field strength decays near the center of the electrode and within the gap between two electrodes.

DEP CHARACTERIZATION

We first characterize the frequency-dependent DEP behaviors of yeast and bacterial cells by varying ac frequencies ranging from 10 kHz to 80 MHz. The cell samples were suspended in either DI water (2 μS/cm) or a NaCl solution (380 μS/cm) to investigate the effect of medium conductivity.

Characterization of Yeast Cells. Figure 4a,b shows yeast cells suspended in a 380 μS/cm NaCl solution are subject to an ac electric field and in the absence of fluid flow. Imposing an ac voltage of 10 V at 10 kHz to the first and third AgPDMS electrodes

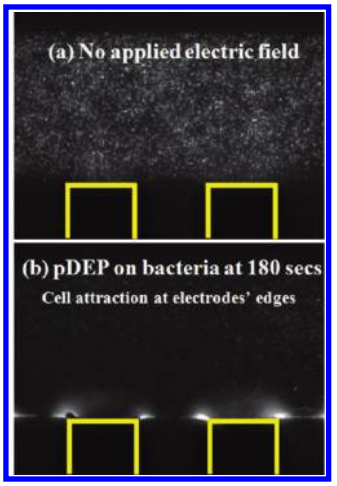

Figure 5. DEP characterization of *E. coli* in a 380 μS/cm NaCl solution. (a) No applied electric field. (b) pDEP-induced attraction of *E. coli* under 15.3 V at 1 MHz.

caused repulsive forces (nDEP) on the yeast cells and their movement away from the electrodes (Figure 4a). This indicates that cells are less polarizable than the suspending medium at low frequency. In contrast, at 10 MHz, yeast cells experienced strong attractive forces (pDEP), moving toward and accumulating at the electrodes' edges (Figure 4b). At 80 MHz, no DEP response was observed. This was expected because at very high frequencies the difference in the complex permittivities of cells and medium (which determines the CM factor) becomes insignificant, thereby causing DEP to vanish. Furthermore, the crossover frequency from nDEP to pDEP was found to be ~300 kHz and the crossover frequency from pDEP to no DEP was ~40 MHz. All these experimental observations are in good agreement with the predictions in Figure 2a.

According to eq 2, when the conductivity of the medium is low enough compared to the conductivity of the cells, the DEP behavior of cells can be inverted from nDEP to pDEP. Our experimental results confirmed this prediction: yeast cells in DI water (2 μS/cm) experience pDEP for all frequencies up to a crossover frequency of 40 MHz, above which no motion of yeast cells was observed as DEP became too weak (refer to the dashed line in Figure 2a). In DI water, yeast cells may experience osmotic pressure but they were alive.[28] Interestingly, yeast cells can form chains when exposed to a nonuniform electric field,[10] and the formation of chains appeared in the same direction as the field lines shown in Figure 3.

Characterization of Bacterial Cells. *E. coli* exhibited similar DEP behaviors as yeast cells in the 380 μS/cm NaCl solution. Weak pDEP was found at 400 kHz and 30 MHz but relatively strong pDEP at 1 MHz. Figure 5a shows *E. coli* in the NaCl solution in the absence of an electric field. An application of 15.3 V at 1 MHz resulted in the pDEP-induced attraction of bacteria at the edges of electrodes (Figure 5b). Two crossover frequencies were identified as 150 kHz (from no DEP to pDEP) and 35 MHz (from pDEP to no DEP). These DEP behaviors are in reasonably good agreement with the prediction from Figure 2b, although below 150 kHz and above 35 MHz no DEP was observed. Furthermore, *E. coli* suspended in DI water always exhibited pDEP at frequencies from 10 kHz to 30 MHz, with a crossover frequency of 35 MHz. Chain formation was also observed.

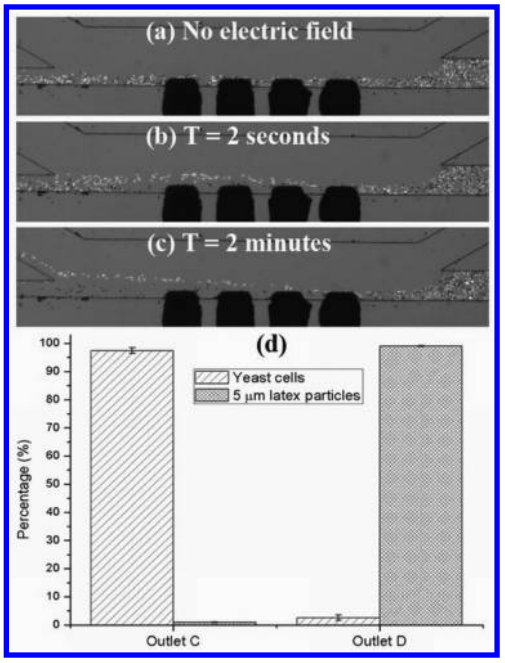

Figure 6. Snapshot images of separating yeast cells (dark dots) from 5 μm latex particles (white dots). (a) Without electric field. (b,c) With an ac voltage of 31.2 V at 300 kHz. Clear separation can be seen after 2 s and 2 min. (d) Separation efficiency of yeast cells and 5 μm latex particles. Images were acquired with a 5× objective (see Movie S1 in the Supporting Information).

The two crossover frequencies of *E. coli* and yeast cells suspended in the 380 μS/cm NaCl solution were rather similar. However, at 10 kHz yeast cells underwent nDEP whereas *E. coli* exhibited pDEP, indicating that yeast cells are in general less conductive than *E. coli*. As indicated by eqs 1 and 2 in the Supporting Information, different size ratios of the cell wall, membrane, cytoplasm, and nucleus can alter the CM factor and thus the crossover frequencies. Moreover, as cytoplasm of both cell types have much higher electrical conductivities than the suspending medium, DEP characterization showed strong pDEP under medium-to-high frequencies (e.g., 500 kHz−10 MHz).

SEPARATION OF YEAST CELLS FROM 5 μm LATEX PARTICLES

On the basis of the prediction that yeast cells and latex particles have distinct DEP responses at frequencies ranging from 300 kHz to 1 MHz in a 380 μS/cm NaCl solution (Figure 2a), we used the microfluidic device to separate a mixture of yeast cells and 5 μm fluorescent latex particles. The particle size was chosen to be close to that of the cells to eliminate size-dependent effects.

Figure 6a shows a snapshot image for yeast cells (black dots) and fluorescent latex particles (white dots) in a continuous flow, in the absence of electric field: cells and particles are hydrodynamically focused near the channel wall with AgPDMS electrodes. After applying 31.2 V at 300 kHz (the crossover frequency), clear separation was observed even after 2 s and remained reliable after 2 min (Figure 6b,c). The particles were pushed away from the electrodes by nDEP. In contrast, the yeast cells experienced weak pDEP and were attracted even further toward the electrodes (the reason yeast cells experienced weak pDEP rather than no DEP is that 300 kHz is close to the

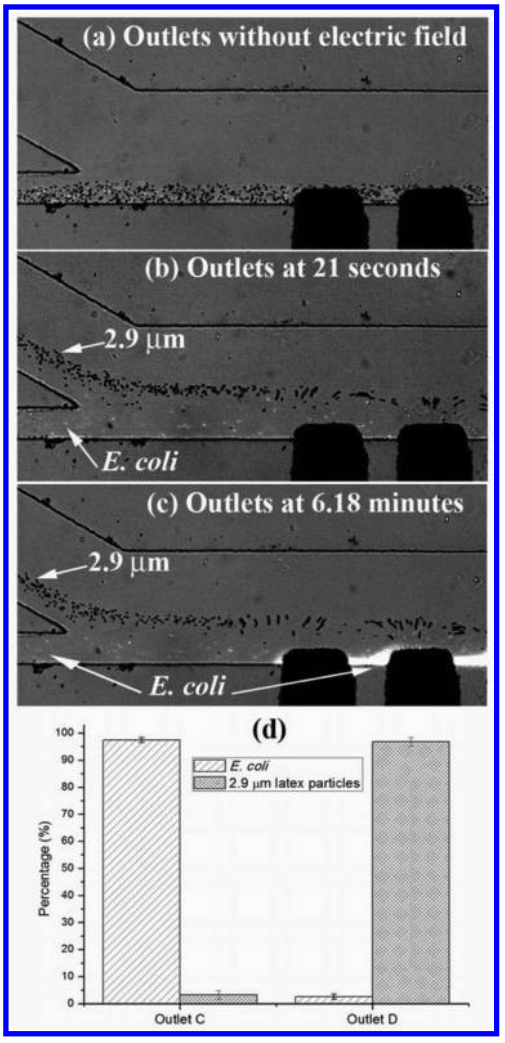

Figure 7. Snapshot images of continuously separating *E. coli* cells and 2.9 μm latex particles. (a) The mixture of samples at outlets with no applied electric field. Separation achieved by applying an ac field of 40.4 V with 1 MHz (b) at 21 s and (c) at 6.18 min. (d) Separation efficiency. Images were acquired with a 10× objective (see Movie S2 in the Supporting Information).

crossover frequency (Figure 2a), and the sign of the DEP force is thus highly sensitive to small frequency variations in this regime). As a result, the yeast cells ended up preferentially in outlet C and the particles in outlet D (Figure 6d), with a separation efficiency >97% (see movie S1 in the Supporting Information). For these experiments, the time window set by the speed of the flow (306 μm/s) and the channel length (1400 μm) was ~4.6 s, thus giving a nDEP drift velocity of ~11 μm/s. The separation of yeast cells (throughput ~780/min) and 5 μm latex particles (throughput ~1200/min) were reliably continued for >5 min at the flow rate of 0.15 μL/min.

SEPARATION OF *E. COLI* FROM 2.9 μm LATEX PARTICLES

Separation of *E. coli* and 2.9 μm latex particles in a 380 μS/cm NaCl solution was also successfully achieved. Figure 7a shows a snapshot image for a stream of *E. coli* and particles which was again focused near the wall, in the absence of electric field. According to the predicted CM factor (Figure 2b), the frequency

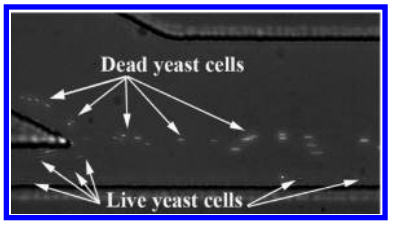

Figure 8. Separation of live and dead yeast cells by applying 26.5 V at 1 MHz.

of 10 MHz is most suitable to separate *E. coli* and the particles, because it leads to strong pDEP for *E. coli* and strong nDEP for particles. However, generation of a higher voltage (40.4 V) limited the maximum frequency attainable by our amplifier to 1 MHz. Even so, clear separation was obtained (Figure 7b,c) with a throughput of 1440 particles/min and 780 cells/min at the flow rate of 0.06 μL/min and very high separation efficiency (Figure 7d) (see Movie S2 in the Supporting Information). For these experiments, the time window set by the speed of the flow (123 μm/s) and the channel length (1400 μm) was ~11.4 s, thus giving a nDEP drift velocity of ~4.4 μm/s.

SEPARATION OF LIVE AND DEAD YEAST CELLS

Here, we tested our device by separating live and dead yeast cells in a 600 μS/cm NaCl solution, based on their difference in electrical properties. When a cell dies, the cell's membrane becomes permeable and allows content in the inner parts of the cell to exchange with external medium.[29] Huang et al. found that the conductivity of the live yeast cell's nucleus which is 0.2 S/m significantly reduces to 7×10^{-3} S/m when it dies.[26] As a result, the dead cell becomes much less conductive and prone to experience nDEP as compared to the live cells. In line with these findings, we observed that at 1 MHz live cells experienced pDEP, whereas dead ones exhibited nDEP. By imposing 26.5 V at 1 MHz, continuous separation of live (black dots) from dead (white dots) yeast cells was successfully achieved at 0.087 μL/min with a throughput of 480 cells/min for both (Figure 8). The separation efficiency was >97%. For these experiments, the time window set by the speed of the flow (181 μm/s) and the channel length (1400 μm) was ~7.7 s, thus giving a nDEP drift velocity of ~6.5 μm/s.

CONCLUSIONS

We have presented a PDMS microfluidic device that can utilize ac-DEP via 3D AgPDMS composites as sidewall electrodes for cell characterization and continuous separation of particles and cells of similar sizes. The device has been used to characterize the DEP properties in terms of pDEP, nDEP, and crossover frequencies for yeast cells and *E. coli*. In addition, the device also has been demonstrated for the continuous separation of yeast cells from similar-size 5 μm latex particles, *E. coli* from similar-size 2.9 μm latex particles, and live yeast cells from dead yeast cells. The successful validation and the high separation efficiency (>97%) make this a promising device in a broad number of applications and a very good candidate for integration in more complex lab-on-chip platforms for biomedical analysis.

■ ASSOCIATED CONTENT

Supporting Information. Additional information and two movies as mentioned in the text. This material is available free of charge via the Internet at http://pubs.acs.org.

■ AUTHOR INFORMATION

Corresponding Author
*Fax: (+65) 6792-4062. E-mail: mcyang@ntu.edu.sg.

■ ACKNOWLEDGMENT

The authors gratefully acknowledge a research grant (Grant AcRF RG 9/07) from the Ministry of Education of Singapore and the Ph.D. Scholarship from Nanyang Technological University. R.S. was supported by NIH Grant 1-R21-EB008844 and NSF Grant OCE-0744641-CAREER.

■ REFERENCES

(1) Wolff, A.; Perch-Nielsen, I. R.; Larsen, U. D.; Friis, P.; Goranovic, G.; Poulsen, C. R.; Kutter, J. P.; Telleman, P. *Lab Chip* **2003**, *3*, 22–27.
(2) Yager, P.; Edwards, T.; Fu, E.; Helton, K.; Nelson, K.; Tam, M. R.; Weigl, B. H. *Nature* **2006**, *442*, 412–418.
(3) Lewpiriyawong, N.; Yang, C.; Lam, Y. C. *Biomicrofluidics* **2008**, *2*, 034105.
(4) Rosenthal, A.; Voldman, J. *Biophys. J.* **2005**, *88*, 2193–2205.
(5) Lapizco-Encinas, B. H.; Simmons, B. A.; Cummings, E. B.; Fintschenko, Y. *Electrophoresis* **2004**, *25*, 1695–1704.
(6) Song, H.; Mulukutla, V.; James, C. D.; Bennett, D. J. *J. Micromech. Microeng.* **2008**, 18.
(7) Shafiee, h.; Sano, M. B.; Henslee, E. A.; Caldwell, J. L.; Davalos, R. V. *Lab Chip* **2010**, *10*, 438–445.
(8) Park, J.; Kim, B.; Choi, S. K.; Hong, S.; Lee, S. H.; Lee, K.-l. *Lab Chip* **2005**, *5*, 1264–1270.
(9) Jung, J.-Y.; Kwak, H.-Y. *Anal. Chem.* **2007**, *79*, 5087–5092.
(10) Jones, T. B. *Electromechanics of Particles*; Cambridge University Press: Cambridge, U.K., 1995.
(11) Lewpiriyawong, N.; Yang, C.; Lam, Y. C. *Electrophoresis* **2010**, *31*, 2622–2631.
(12) Kang, Y.; Li, D.; Kalams, S. A.; Eid, J. E. *Biomed. Microdevices* **2008**, *10*, 243–249.
(13) Markx, G. H.; Talary, M. S.; Pethig, R. *J. Biotechnol.* **1994**, *32*, 29–37.
(14) Markx, G. H.; Rousselet, J.; Pethig, R. *J. Liq. Chromatogr. Related Technol.* **1997**, *20*, 2857–2872.
(15) Morgan, H.; Izquierdo, A. G.; Bakewell, D.; Green, N. G.; Ramos, A. *J. Phys. D: Appl. Phys.* **2001**, *34*, 1553.
(16) Iliescu, C.; Xu, G. L.; Samper, V.; Tay, F. E. H. *J. Micromech. Microeng.* **2005**, *15*, 494–500.
(17) Park, B. Y.; Madou, M. J. *Electrophoresis* **2005**, *26*, 3745–3757.
(18) Wang, L.; Flanagan, L.; Jeon, N. L.; Monuki, E.; Lee, A. P. *Lab Chip* **2007**, *7*, 1114–1120.
(19) Tay, F. E. H.; Yu, L.; Pang, A. J.; Iliescu, C. *Electrochim. Acta* **2007**, *52*, 2862–2868.
(20) Iliescu, C.; Tresset, G.; Xu, G. *Biomicrofluidics* **2009**, *3*, 044104.
(21) Xia, Y.; Whitesides, G. M. *Annu. Rev. Mater. Sci.* **1998**, *28*, 153–184.
(22) Niu, X.; Peng, S.; Liu, L.; Wen, W.; Sheng, P. *Adv. Mater.* **2007**, *19*, 2682–2686.
(23) Cetin, B.; Kang, Y.; Wu, Z.; Li, D. *Electrophoresis* **2009**, *30*, 766–772.
(24) Kang, Y.; Cetin, B.; Wu, Z.; Li, D. *Electrochim. Acta* **2009**, *54*, 1715–1720.
(25) Morgan, H.; Green, N. G. *AC Electrokinetics: Colloids and Nanoparticles*; Research Studies Press: Philadelphia, PA, 2003.
(26) Huang, Y.; Holzel, R.; Pethig, R.; Wang, X.-B. *Phys. Med. Biol.* **1992**, *37*, 1499–1517.
(27) Suehiro, J.; Hamada, R.; Noutomi, D.; Shutou, M.; Hara, M. *J. Electrostatics* **2003**, *57*, 157–168.
(28) Wolfson, A.; Haddad, N.; Dlugy, C.; Tavor, D.; Shotland, Y. *Org. Commun.* **2008**, *1*, 9–16.
(29) Tay, F. E. H.; Yu, L.; Panga, A. J.; Iliescu, C. *Electrochim. Acta* **2007**, *52*, 2862–2868.